encit 2020

ABCM Associação Brasileira de Engenharia e Ciências Mecânicas

18th Brazilian Congress of Thermal Sciences and Engineering
November 16–20, 2020 (Online)

ENC-2020-0406
NUMERICAL SOLUTION OF THE FLOW CONTROL IN A BACKWARD-FACING STEP FOR VARIOUS REYNOLDS NUMBERS

Deidson Vilhena Santos
Álvaro Luis de Bortoli
Federal University of Rio Grande do Sul - UFRGS. Av. Bento Gonçalves, 9500 - Agronomia, Porto Alegre - RS, 90650-001.
deidsonjc@hotmail.com; dbortoli@mat.ufrgs.br

Abstract. *The Backward-Facing Step flows have been widely studied aiming optimization of flows and, most recently, control strategies have been applied for it. So, in this work a numerical investigation of the effect of a closed-loop control for a flow in a backward-facing step, whose expansion ratio is 3.0, is given. The flow equations are the incompressible set of Navier-Stokes equations, while the control equations are given in the state-space formulation. The flow solution is obtained via Computational Fluid Dynamics using the Runge-Kutta method, where the equations are discretized by centered finite differences scheme. The analysis is given for four Reynolds numbers (*50*,* 100*,* 300 *and* 500*) whose recirculation zone and instabilities increase considerably as* Re *increases. The results of the flow fields have been validated with data from the literature, through the length of the recirculation zone and the vorticity fields, obtaining good agreement in the comparisons. In the investigation of the effect of the control applied on the flow, it was noted the characterization of an oscillatory profile, obtaining: better and more efficient mixing pattern; anticipation of 12.43% at x-position of the point of reattachment; 18.9% reduction in the length of the recirculation zone; and 753.23% increase in the flow speed at a pre-established point.*

Keywords: *Backward-Facing Step, Navier-Stokes Equations, Closed-Loop Control, Computational Fluid Dynamics.*

1. INTRODUCTION

In the last two decades the fluid dynamics has been widely applied to different science fields. Such studies were potentialized with the emergence of Computational Fluid Dynamics (CFD) (Ferziger *et al.*, 2002). This made possible a wider range of simulations, which would previously have a very high cost to be done experimentally.

Such applications include climate predictions (Sigalotti *et al.*, 2014), aerospace industry (Spalart and Venkatakrishnan, 2016), aerodynamic drag force in vehicles and aircrafts (McCallen *et al.*, 2013; Ghoreyshi *et al.*, 2009), transportation of oils by pipelines in the petrochemical industry (Zambrano *et al.*, 2017; Desamala *et al.*, 2014), hemodynamics analysis in the carotid artery and cardiovascular medicine (Qian *et al.*, 2007; Morris *et al.*, 2016), and still, the study of the dynamics of fire and other natural phenomena aiming the reproduction of more realistic visual effects in the cinematographic and electronics games industries (Nguyen *et al.*, 2003).

The Backward-Facing Step (BFS) flow is a branch of fluid dynamics that has been widely studied recently by its applications in engineering problems characterizing a similar geometric domain to that these problems have (Montazer *et al.*, 2018). Therefore, despite its simple geometry, BFS flows serve as prototypes to investigate flow characteristics such as the flow stabilization, the shear layer, the recirculation zone, the boundary layer separation and the mixing pattern (Liakos and Malamataris, 2015). For example, the influence of different expansion ratios to various Reynolds numbers over the recirculation zone length was numerically studied in a BFS flow by Biswas *et al.* (2004). A numerical investigation was done by Choi *et al.* (2016), aiming the detailed analysis of the influence of various angles of inclination of the step over the location of the reattachment point of the BFS flow. The effect of the Reynolds number variation over the flow field has been numerically analyzed, where is observed a significant variation in the flow mixing pattern as Re increases (Hossain *et al.*, 2013; Nowruzi *et al.*, 2018). In addition, the properties of non-Newtonian fluid flows (Ameur and Menni, 2019) and turbulent flows (Anwar-ul Haque *et al.*, 2007; Wu *et al.*, 2013) have been studied in BFS flows.

Furthermore, different control strategies have been applied to BFS flow with the aim to get an enhancement in the flow properties. An active control in a BFS is given in Coskun *et al.* (2016), by the injection of a jet in the duct's upper wall, simultaneously to a suction at the lateral wall of the step, obtaining a reduction in the recirculation zone length. In Bolgar *et al.* (2016), a passive control is applied to a BFS flow through the variation of step peak size, obtaining a 25% reduction in the distance from the reattachment point to the step. Plasma actuators have been used to perform an active control of BFS flows, showing good effectiveness to change the flow properties (D'Adamo *et al.*, 2014; Wang and Li, 2016).

Most recently, through of heating the step and duct walls, the effects of heat transfer between the walls and the fluid

in BFS flows have been analyzed (Chen *et al.*, 2018; Hilo *et al.*, 2020a; Li *et al.*, 2019). The effect of nanofluids in BFS flows also have been studied with the aim of get an enhancement in the heat transfer between the fluid and the wall, where such effect is potentialized by the properties of nanoparticles present in the base fluid (Salman *et al.*, 2019; Hilo *et al.*, 2020b). An enhancement of combustion processes has been achieved both, via numerical investigations about the effect of the dispersion of nanoparticles in base fuels, namely, nanofuels (Nong *et al.*, 2020; Edam and Al-Dawody, 2019), and through the study of flows over BFS combustors (Pillai *et al.*, 2020; Huang *et al.*, 2016), simulating the real behavior of engines, turbines, among others.

In all applications of BFS cited previously, the results depend directly of the flow properties that occurs in this geometry. For example, the literature results showed that the effects of heat transfer are most effective in the region behind the step, namely the recirculation zone; therefore, a significantly alteration in this region can change the effectiveness of this process. Also, to occur an effective combustion process of nanofuels or in combustors, is necessary an efficient mixing of the reagents. Therefore, the characteristics of mixing pattern of the flow have paramount importance to an efficient combustion. In addition, in the pipeline transport and in the carotid artery flux, it is necessary a flow well developed, with a good flux in the shear layer to maintain good intensity of the speed in this region.

For this reason, in this paper a control strategy to improve these properties of BFS flow was developed. How can be seen in the literature, only one of these flow properties was analyzed in each work: recirculation zone length, flow velocity and mixing pattern. Therefore, the main objective of this work is to develop an effective mathematical-computational model for active control in a BFS flow, through a simultaneous action of injection/suction, with the purpose to improve at same time the flow properties cited previously. The validation of the mathematical model of this work will be by the comparison of the flow fields and of the recirculation zone length with results of the literature (Nowruzi *et al.*, 2018; Biswas *et al.*, 2004). At last, the effect of the control over the BFS flow is investigated.

2. MATHEMATICAL MODELING

2.1 Backward-Facing Step Geometry

Figure 1 shows the geometric domain which is subject of study in this work. Such geometry is called *backward-facing step* (BFS), where the parameters showed in the figure, with its proportions, were taken according to the work of Nowruzi *et al.* (2018). The key parameter of this geometry is the length value h_i, of which all other dimensions are taken, which represents the height of the inflow of the channel. The step height is given by $h_s = 2h_i$, the step width is $L_1 = 5h_i$, the distance from the step to the end of the duct, is given by $L_0 = 30h_i$, and the height of the duct is given by $H = h_s + h_i$.

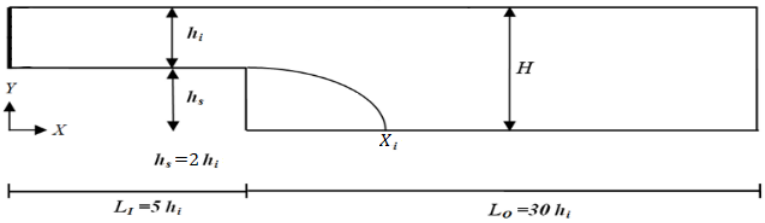

Figure 1: Backward-Facing Step Geometry.

In this work, we establish $h_i = 1.0$, therefore, in Fig. 1 the geometry will assume the following values: $h_s = 2.0$; $L_1 = 5.0$; $L_0 = 30.0$ and $H = 3.0$. In BFS models, there is the relation $\frac{H}{h_i}$ called *expansion ratio*. In this work $\frac{H}{h_i} = 3.0$.

Still in Fig. 1, we highlight the curved trace behind the step, which represents the *recirculation zone*, which is formed because of the separation of the flow in the edge of the step. After detaching in the edge of the step, the fluid descends, until touching the base, whose point X_i is called *reattachment point*, which characterizes the recirculation zone length.

2.2 Flow Equations

The equations of the flow are given by the set of the dimensionless incompressible Navier-Stokes equations, that are the continuity and momentum equations:

$$\vec{\nabla} \cdot \vec{u} = 0 \,, \tag{1}$$

$$\frac{\partial \vec{u}}{\partial t} + \vec{u}\vec{\nabla}\vec{u} = -\vec{\nabla}p + \frac{1}{Re}\vec{\nabla}^2\vec{u} \,, \tag{2}$$

where $\vec{u}$ is the vector of velocity of the flow, p is the pressure and Re is the Reynolds number, the dimensionless number relating inertial forces and viscous forces of the flow, which is given by $Re = \dfrac{\rho V L}{\mu}$. Here ρ, V, L and μ are, respectively,

the specific mass of the fluid, the average velocity of the inlet flow, the diameter of the inlet and the dynamic viscosity of the fluid.

The pressure equation was derived obtaining a Poisson equation model, according to Beleza (2003), that is given, making $D = u_x + v_y$ as the continuity equation, by:

$$\vec{\nabla}^2 p = -\left[u_x u_x + 2u_y v_x + v_y v_y\right] - D_t + \frac{1}{Re}\left(D_{xx} + D_{yy}\right) \ . \tag{3}$$

Lastly, the relation for vorticity ω will be applied according to the model given by Hughes and Brighton (1967):

$$\omega = \frac{1}{2}\left(\frac{\partial v}{\partial x} - \frac{\partial u}{\partial y}\right) \ . \tag{4}$$

2.3 State-Space Formulation

The control strategy applied in the flow is given by a system of ordinary differential equations; this system is called *state-space formulation*. The model used in this work is given according to Schmid (2009):

$$\dot{x}(t) = A\vec{x}(t) + B\vec{u}(t) \ , \tag{5}$$

$$\vec{y}(t) = C\vec{x}(t) \ , \tag{6}$$

where the Eq. 5 describes the full state of the flow with the control action, while the Eq. 6 gives the measure of the observer in this flow.

The $\vec{x}(t)$ vector is the *state vector* of the flow, namely, is the vector formed by the state variables of the problem. The matrix A denotes the *states matrix*, which can be approximated by the Jacobian matrix of the linearized Navier-Stokes equations. The matrix B denotes the positions of the actuators, and $\vec{u}(t)$ is the action of control. The measure of the flow is denoted for $\vec{y}(t)$, where the matrix C determines the observer position.

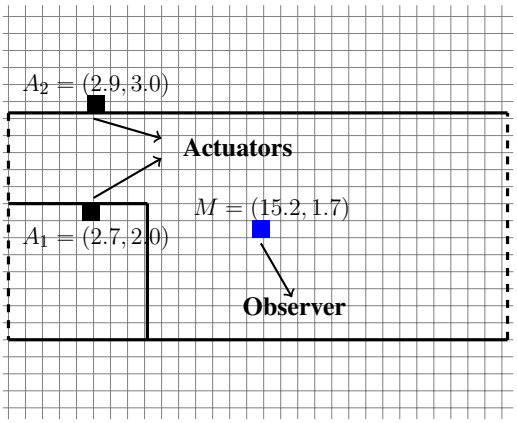

Figure 2: Positions of the actuators and observer in the BFS flow.

In Fig. 2, the positions of the actuators and observer are shown. The observer, in the position M, computes the measure in the flow and sends the information to the actuators, in the positions A_1 and A_2, that update their values and perform a simultaneous action of injection/suction in the same direction, depending on the value of the measure sent by the observer.

This process is called *closed-loop control*, where both injection and suction of the actuators are performed in the wall-normal direction. Such action has achieved more efficacy in flow control than actions in wall-tangential directions (Yim *et al.*, 2019).

2.4 Initial and Boundary Conditions

The initial conditions were taken in such a way that the pressure is given by the atmospheric pressure and the velocity of the flow is taken as a regime hydrodynamically fully developed. This behavior is given by a parabolic profile at x-direction in the time $t = t_0$, according at Besanjideh *et al.* (2016):

$$u(t_0) = 6y(1 - y) \ ; \tag{7}$$

$$v(t_0) = 0 \ ; \tag{8}$$

$$p(t_0) = p_0 = 10^5 \ . \tag{9}$$

The boundary conditions are taken for duct and step walls being considered adiabatic and impermeable. Hence, for velocities, at the top and bottom walls, no-slip conditions are imposed, at the inlet parabolic condition and at the output extrapolation is imposed. For pressure, at the inlet its initial value is fixed and extrapolation is taken for all other walls. In the step, no-slip for velocities and extrapolation for pressure are imposed. Figure 3 shows these boundary conditions in the BFS.

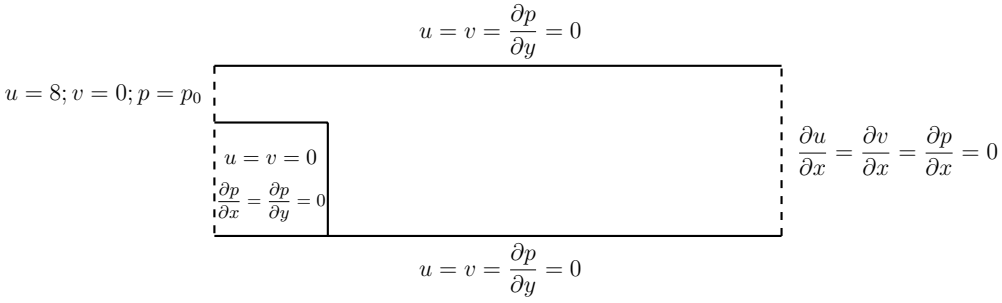

Figure 3: Boundary conditions for the backward-facing step flow.

3. NUMERICAL SOLUTION PROCEDURES

3.1 Computational Mesh

Figure 4 shows a representation of the computational mesh applied in the numerical simulation of this work. It is giving by a structured grid containing 350×30 points, that is 10,500 cells in total.

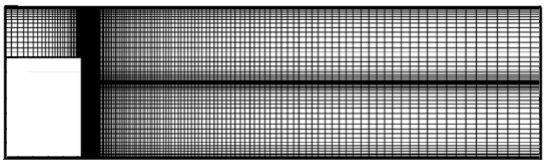

Figure 4: Computational mesh - 350×30 points.

The refinement is given in the edge of the step at the x-direction and in the middle of the duct at the y-direction. This is done because the shear layer formed between the recirculation zone and the upstream is the region of most interest in this work.

3.2 Finite Difference Scheme

The equations of the problem were discretized by the finite difference method, that applies Taylor series approximations for the equations system, according to Ferziger *et al.* (2002). It is used a centered finite difference scheme for the first and second order partial derivatives. For example, the partial derivative in x for an arbitrary variable f is:

$$\begin{aligned}
\left(\frac{\partial f}{\partial x}\right)_{(i,j,k,t)} &= \frac{f_{(i+1,j,k,t)} - f_{(i-1,j,k,t)}}{2\Delta x} + O(\Delta x^2) \\
\left(\frac{\partial^2 f}{\partial x^2}\right)_{(i,j,k,t)} &= \frac{f_{(i+1,j,k,t)} - 2f_{(i,j,k,t)} + f_{(i-1,j,k,t)}}{\Delta x^2} + O(\Delta x^2) \ ,
\end{aligned}$$

where Δx represents the step in x and $O(\Delta x^2)$ is the truncation error.

3.3 Runge-Kutta Method

The numerical method used to obtain the solution of the equations system was the simplified Runge-Kutta method. This method is characterized by the small number of operations required. The use of this scheme is chosen because it requires less computational memory and its coefficients can be selected in order to obtain solutions of high temporal

precision (De Bortoli, 2000). For the system $\frac{\partial \vec{W}}{\partial t} = \vec{R}$, this scheme is given by:

$$\begin{aligned} \overrightarrow{W}_{i,j,k}^{(0)} &= \overrightarrow{W}_{i,j,k}^{(n)} \; ; \\ \overrightarrow{W}_{i,j,k}^{(r)} &= \overrightarrow{W}_{i,j,k}^{(0)} - \alpha_r \Delta t \overrightarrow{R}_{i,j,k}^{(r-1)} \; ; \\ \overrightarrow{W}_{i,j,k}^{(n+1)} &= \overrightarrow{W}_{i,j,k}^{(3)} \; , \end{aligned}$$

where Δt is the step of time used in the numerical simulation, $\overrightarrow{W}$ represents the states of the system and $\overrightarrow{R}$ represents the residue.

The parameter $r = 1, 2, 3$ is the stages number of the method and the coefficients α_r, namely Runge-Kutta's coefficients, are given by $\alpha_1 = 1/2$, $\alpha_2 = 1/2$ and $\alpha_3 = 1$ for second order time accuracy. More than two stages are employed for the purpose of extending the stability region.

4. RESULTS AND DISCUSSION

For the presentation of the results, firstly the validation was done, by mean of the comparison with data from the literature (Nowruzi *et al.*, 2018; Biswas *et al.*, 2004), through the length of the recirculation zone obtained for four different values of the Reynolds number (50, 100, 300 and 500). Next, the vorticity fields for the same values of the Reynolds number were compared with the results of Nowruzi *et al.* (2018).

Finally, the characteristics of the flow field before and after the control will be discussed and compared. In other words, a reference Reynolds number ($Re = 500$) will be fixed, and then, the altered characteristics in the flow field will be synthesized. Such characteristics are the mixing pattern, the speed in the shear layer and the location of the reattachment point.

4.1 Validation of the Methodology

The Reynolds number (Re) is of paramount importance in obtaining the results, because by relating the inertial forces to the viscous forces, its increase generates disturbances, or instabilities, along the flow. As a dimensionless number, it can be changed independently of the units of measurement used and of the dimensions of the geometry. Therefore, for the same established parameters, one can analyze the change of flow properties only by means of the variation of the Reynolds number within a predetermined range.

4.1.1 Recirculation Zone Length

The flow fields resulting of the numerical solution obtained in this work are shown in Fig. 5.

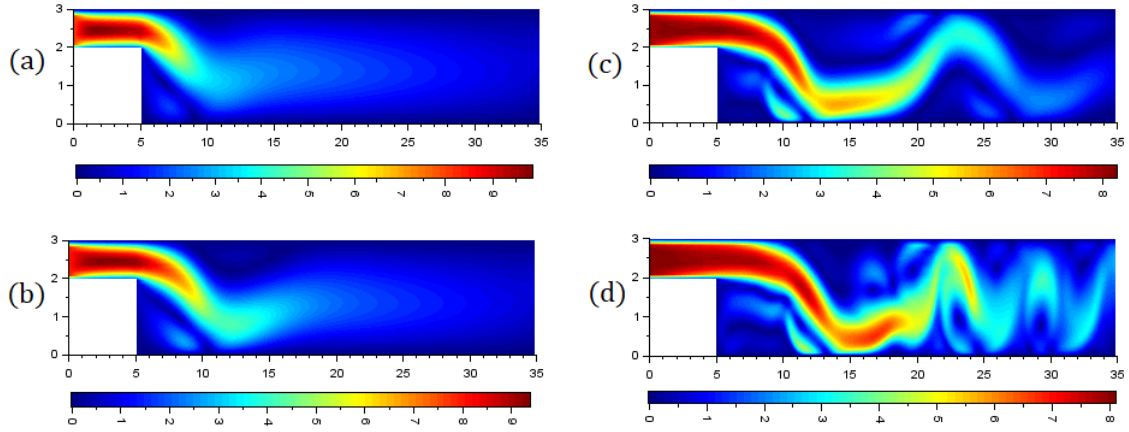

Figure 5: Flow fields for different values of Reynolds number. (a) $Re = 50$, (b) $Re = 100$, (c) $Re = 300$ and (d) $Re = 500$.

Figure 5 shows that both flow instability and recirculation zone length increases as Re increases. For $Re = 50$ and $Re = 100$ the flow remains reasonably stable. For $Re = 300$ instabilities along the flow are observed, which increase for $Re = 500$; consequently, the recirculation zone length increases considerably.

The values obtained in this work for the recirculation zone length are compared in table 1 with results obtained in the literature (Nowruzi *et al.*, 2018; Biswas *et al.*, 2004), for the expansion ratio $\frac{H}{h_i} = 3.0$.

Table 1: Results for recirculation zone length.

Results	Reynolds Number (Re)			
	50	100	300	500
This Work	5.595	6.775	8.405	9.645
Biswas *et al.* (2004)	3.766	6.277	10.744	-
Nowruzi *et al.* (2018)	3.865	6.365	9.685	10.810

As can be noted in the table 1, the results obtained in this work are in reasonable agreement with the results of the literature. Both results reaffirm the fact that the recirculation zone length increases as Re increases, such as could be seen in Fig. 5.

4.1.2 Vorticity Fields

The direct contact of the fluid with the walls and step promotes viscous tensions and generate instabilities in the flow through the formation of vortices. Hence, the distribution of vortices is characterized as one of the determining factors for the flow field, whose description of the vortices structure along the flow is given by the vorticity field.

Therefore, the vorticity field was the object of comparison of the results of this work with the results of Nowruzi *et al.* (2018), obtaining the validation of the mathematical-computational model developed in this work. These comparisons are shown in Fig. 6, where the results were obtained for $Re = 50,\ 100,\ 300$ and 500 .

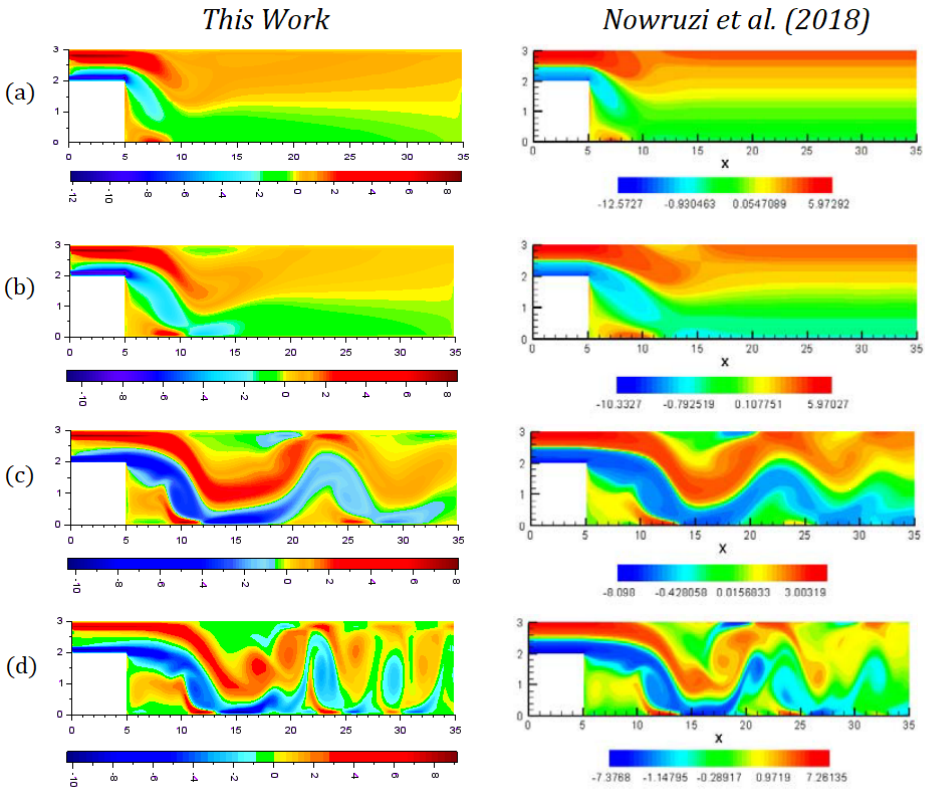

Figure 6: Comparison of the results for the vorticity field ω. (a) $Re = 50$, (b) $Re = 100$, (c) $Re = 300$ e (d) $Re = 500$.

Note that, in the results shown in Fig. 6, immediately after the detachment of the flow on the edge of the step, there is the formation of the shear layer, located between the upstream and the recirculation zone, which extends to the reattachment point. Also, it is identified that the increase of the Reynolds number directly implies the increase of the length of the shear layer, and thus the length of the recirculation zone. Such effects indicate a reasonable similarity between both results.

It is observed, both in the results of this work and in the results of Nowruzi *et al.* (2018), that in the positions relative to the critical points of maximum and minimum oscillation in the flow field, the maximum and minimum magnitudes of the vorticity occur, respectively. This is due to the sudden change of the direction of the flow in these points. The identification of such points in the same locations in both vorticity fields corroborates the agreement between the results.

4.2 Results of the Control

Based on the good performance of the mathematical-computational model, obtained through the comparisons of the results of this work with the results of the literature, this section will develop the analysis of effects of the control strategy of this work over the flow. For this purpose, the value of $Re = 500$ is fixed as Reynolds of reference, because is in this value that can be observed greater oscillation in the flow field and greater velocity in the shear layer (as it can be observed in Fig. 5). In addiction, the majority of physical applications are given for higher values of Re.

4.2.1 Mixing Pattern of the Flow

In the investigation of the flow field before and after the control actuation, through Fig. 7, it is noticed the characterization of a more oscillatory flow due to the control insertion, whose disturbances introduced in the inputs/outputs generate new vortices in the flow.

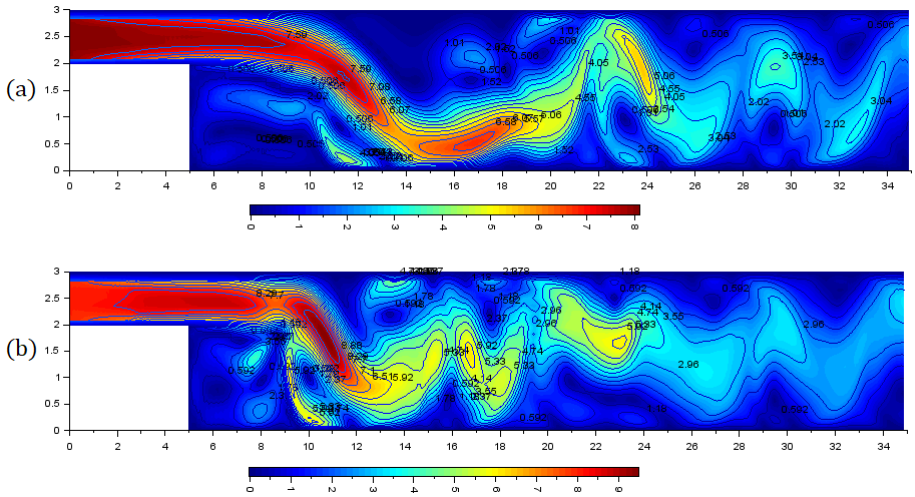

Figure 7: Results of the flow field for $Re = 500$. (a) Without control action and (b) With control action.

Is noticed a decrease in the shear layer length and, hence, the anticipation of the flow development, causing oscillations in upstream locations and, in addition, the emergence of new oscillations in the flow field. This occurrence, of a more oscillatory field, is triggered by the generation of new regions with vortices, because it is in these regions that the changes in the flow direction occur, as can be observed in Fig. 8.

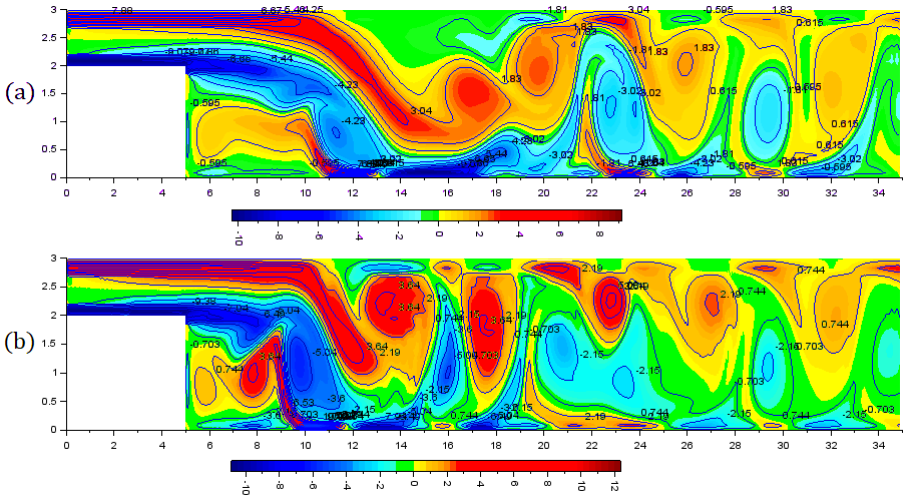

Figure 8: Results of the vorticity field for $Re = 500$. (a) Without control action and (b) With control action.

As a consequence of these new regions with vortices, a region with initially only one large vortex becomes two or more regions with smaller vortices, which give to mass particles greater movement due to their more rapid rotations, which benefits the mixture of fluid particles. The achievement of higher velocity in the vortices can be observed in the increase of the range in the magnitudes bar of Fig. 8, which varied from -10 to 9 before and passed to the range from -11

to 12 after the control action. Therefore, better and more efficient mixing pattern is obtained by means of control strategy.

4.2.2 Velocity in the Shear Layer

In Fig. 9 is shown the velocity field $\vec{u}$ of the flow for $Re = 500$, before and after the control action. A cut-off is given near the point $x = 15$ in the shear layer, where the measurement of the velocity $\vec{u}$ of the flow is taken. This point is given by $M = (15.2, 1.7)$. As shown in Fig. 9 (a), the velocity obtained in the point M is $\vec{u} = 0.622$.

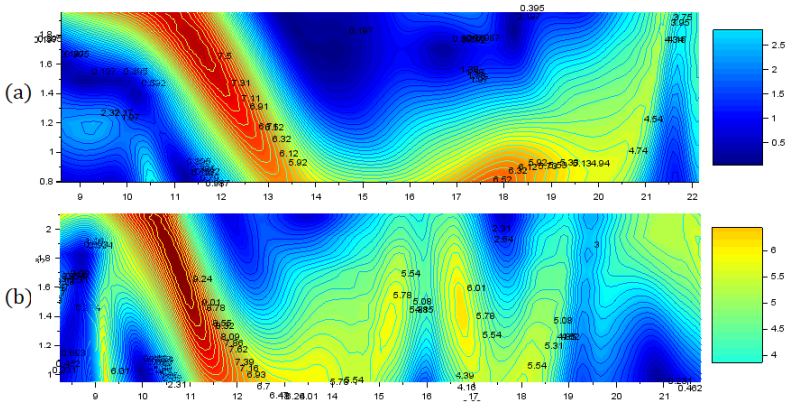

Figure 9: Results of the velocity field for $Re = 500$, near the point $M = (15.2, 1.7)$. (a) Without control action and (b) With control action.

Figure 9 (b) shows the changes in the flow by means of the control, which caused an increase of the velocity in the point M. This new velocity is denoted by $\vec{u}_c$, and its value was $\vec{u}_c = 5.291$.

Therefore, by mean of the application of the control in the flow, it was reached an increase of about 753% in flow velocity at the desired point M.

To reach this value at the point M, the continuous performance of the control was intense enough to change the flow field, obtaining a diminishing of the shear layer, displacing backwards the vortices that were after it. The control modified the recirculation zone, shortening it.

Obtaining higher mixing pattern in the flow field is a direct consequence of the changes done by the control to increase the velocity in the point M. It was seen that such best mixing pattern triggers a greater number of regions with vortices, which are accelerated by mean of increase of the velocity, obtained by the control actuation. In this way, fluid particles are mixed with higher speed and more efficiency.

4.2.3 Reattachment Point

In Fig. 10 is shown the velocity field $\vec{u}$ of the flow for $Re = 500$, but this time in the vicinity of the reattachment point, before and after the control action. In this case, the exact location of the reattachment point is observed, instead of the recirculation zone length. The location of this point in the BFS flow is given by the length of the recirculation zone added to the width of the step.

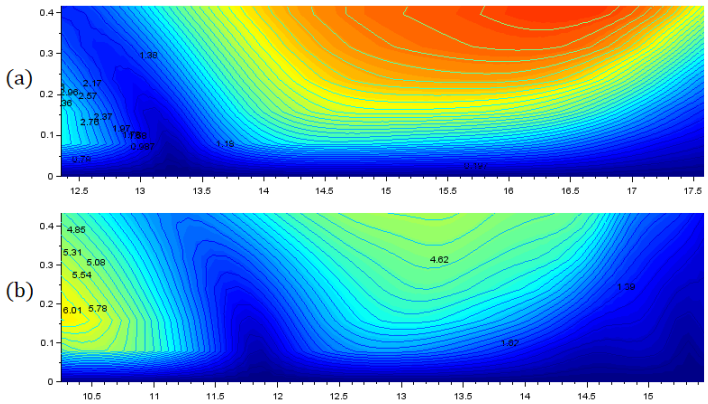

Figure 10: Velocity field for $Re = 500$, near the reattachment point. (a) Without control action and (b) With control action.

Fig. 10 (a) shows the position of the reattachment point in the flow field for $Re = 500$ without control action, that is

given by, $X_i = 14.645$.

In the previous results, it was found that the control action generated anticipation in the development of flow oscillations, with the objective of increasing the flow velocity in the point M. Such anticipation decreased the length of the shear layer. As a consequence, the recirculation zone and the reattachment point were reduced in x. Figure 10 (b) shows the location of the reattachment point after the control action, where such point is denoted by X_c and its location is given by, $X_c = 12.825$.

Therefore, through the application of the mathematical-computational model of this work for the control of the flow over a BFS, it was possible to anticipate in 12.43% the position in x of the reattachment point. Equivalently, we obtained a reduction of 18.9% of the length of the recirculation zone, which characterizes a reasonable reduction, according to the results of Bolgar *et al.* (2016), that obtained a reduction of 25% of the recirculation zone by means of a passive control.

5. CONCLUSION

The coupling of the equations that composed the mathematical-computational model of this work proved to be in good compatibility for obtaining control of the BFS flow. It was obtained good agreement of the results of this work with those from the literature, by the comparison of the recirculation zone length and for the vorticity fields, where the analysis was given for four values of the Reynolds number: 50, 100, 300, and 500. Such results culminated in good validation of the mathematical-computational model applied in this work.

For the synthesis of the results after the performance of the control, was taken $Re = 500$ as Reynolds of reference. A 12.43% anticipation in the position in x of the reattachment point of the flow was obtained. Equivalently, it was obtained a reduction of 18.9% of the recirculation zone length located behind the step, which characterizes a reasonable reduction, according to the results of the literature.

Finally, the good effectiveness of the control actuation caused the increase of the velocity near the point M where the measure was made in the flow. Thus, an increase of approximately 753% in the flow velocity in the desired point M by means of the control strategy employed in this work was obtained.

Despite of its simple geometry, Backward-Facing Step Flows serve as prototype for problems of optimization of flow properties such as boundary-layer separation, flow instabilities, sudden expansion, among others. Because of this, this work developed a numerical solution that can be applied in the optimization, for example, of the mixing of combustion processes in combustors, of the velocity in pipelines transport, of the effect of the lift and drag forces, of the heat transfer effect on coolings and heat exchangers, of heat transfer in nanofluids and of combustion process in nanofuels.

6. REFERENCES

Ameur, H. and Menni, Y., 2019. "Non-newtonian fluid flows through backward-facing steps". *SN Applied Sciences*, Vol. 1, No. 12, p. 1717.

Anwar-ul Haque, F.A., Yamada, S. and Chaudhry, S.R., 2007. "Assessment of turbulence models for turbulent flow over backward facing step". In *Proceedings of the World Congress on Engineering*. Vol. 2, pp. 2–7.

Beleza, L.C., 2003. *Simulação de Movimento Sanguíneo na Artéria Carótida Usando Diferenças Finitas*. Dissertação de Mestrado, PPGMAP: Universidade Federal do Rio Grande do Sul.

Besanjideh, M., Hajabdollahi, M. and Nassab, S.A.G., 2016. "CFD based analysis of laminar forced convection of nanofluid separated flow under the presence of magnetic field". *Journal of Mechanics*, Vol. 32, No. 6, pp. 777−785.

Biswas, G., Breuer, M. and Durst, F., 2004. "Backward-facing step flows for various expansion ratios at low and moderate Reynolds numbers". *Journal of Fluids Engineering*, Vol. 126, No. 3, pp. 362−374.

Bolgar, I., Scharnowski, S. and Kähler, C.J., 2016. "Control of the reattachment length of a transonic 2D backward-facing step flow". In *Proceedings of the 5th International Conference on Jets, Wakes and Separated Flows*. Springer, pp. 241−248.

Chen, L., Asai, K., Nonomura, T., Xi, G. and Liu, T., 2018. "A review of backward-facing step (bfs) flow mechanisms, heat transfer and control". *Thermal Science and Engineering Progress*, Vol. 6, pp. 194–216.

Choi, H.H., Nguyen, J. and Nguyen, V.T., 2016. "Numerical investigation of backward facing step flow over various step angles". *Procedia Engineering*, Vol. 154, pp. 420–425.

Coskun, U.C., Cadirci, S. and Gunes, H., 2016. "Active flow control behind a backward facing step using a zero-net-mass-flux system". In *Proceedings of the 5th International Conference on Jets, Wakes and Separated Flows*. Springer, pp. 231−239.

D'Adamo, J., Sosa, R. and Artana, G., 2014. "Active control of a backward facing step flow with plasma actuators". *Journal of Fluids Engineering*, Vol. 136, No. 12, pp. 1−37.

De Bortoli, A.L., 2000. *Introdução à Dinâmica de Fluidos Computational*. Ed. Universidade/UFRGS.

Desamala, A.B., Dasamahapatra, A.K. and Mandal, T.K., 2014. "Oil-water two-phase flow characteristics in horizontal pipeline - a comprehensive CFD study". *International Journal of Chemical, Molecular, Nuclear, Materials and Metallurgical Engineering*, Vol. 8, No. 4, pp. 360−364.

Edam, M.S. and Al-Dawody, M.F., 2019. "Effect of nano fuel additives on the characteristics of diesel engine fed with biodiesel blended fuel". *Journal of University of Babylon for Engineering Sciences*, Vol. 27, No. 4, pp. 124–141.

Ferziger, J.H., Perić, M. and Street, R.L., 2002. *Computational Methods for Fluid Dynamics*, Vol. 3. Springer-Verlag.

Ghoreyshi, M., Da Ronch, A., Badcock, K., Dees, J., Berard, A. and Rizzi, A., 2009. "Aerodynamic modelling for flight dynamics analysis of conceptual aircraft designs". In *27th AIAA Applied Aerodynamics Conference*. p. 4121.

Hilo, A.K., Iborra, A.A., Sultan, M.T.H., Hamid, M.F.A. *et al.*, 2020a. "Effect of corrugated wall combined with backward-facing step channel on fluid flow and heat transfer". *Energy*, Vol. 190, p. 116294.

Hilo, A.K., Iborra, A.A., Sultan, M.T.H., Hamid, M.F.A. *et al.*, 2020b. "Experimental study of nanofluids flow and heat transfer over a backward-facing step channel". *Powder Technology*, Vol. 372, pp. 497–505.

Hossain, M.A., Rahman, M.T. and Ridwan, S., 2013. "Numerical investigation of fluid flow through a 2d backward facing step channel". *International Journal of Engineering Research & Technology*, Vol. 2, No. 10, pp. 3700–3708.

Huang, W., Li, L.q., Yan, L. and Liao, L., 2016. "Numerical exploration of mixing and combustion in a dual-mode combustor with backward-facing steps". *Acta Astronautica*, Vol. 127, pp. 572–578.

Hughes, W.F. and Brighton, J.A., 1967. *Fluid Dynamics:[includes 100 solved problems]*. Schaum Publishing Co.

Li, Z., Guo, S., Bai, H. and Gao, N., 2019. "Combined flow and heat transfer measurements of backward facing step flows under periodic perturbation". *International Journal of Heat and Mass Transfer*, Vol. 130, pp. 240–251.

Liakos, A. and Malamataris, N.A., 2015. "Topological study of steady state, three dimensional flow over a backward facing step". *Computers & Fluids*, Vol. 118, pp. 1–18.

McCallen, R., Browand, F. and Ross, J., 2013. *The Aerodynamics of Heavy Vehicles: trucks, buses, and trains*. Springer–Verlag Berlin Heidelberg.

Montazer, E., Yarmand, H., Salami, E., Muhamad, M.R., Kazi, S. and Badarudin, A., 2018. "A brief review study of flow phenomena over a backward-facing step and its optimization". *Renewable and Sustainable Energy Reviews*, Vol. 82, pp. 994–1005.

Morris, P.D., Narracott, A., von Tengg-Kobligk, H., Soto, D.A.S., Hsiao, S., Lungu, A., Evans, P., Bressloff, N.W., Lawford, P.V., Hose, D.R. *et al.*, 2016. "Computational fluid dynamics modelling in cardiovascular medicine". *Heart*, Vol. 102, No. 1, pp. 18−28.

Nguyen, D., Enright, D. and Fedkiw, R., 2003. "Simulation and animation of fire and other natural phenomena in the visual effects industry". In *Western States Section, Combustion Institute, Fall Meeting, UCLA*.

Nong, H., Hajizadeh, M.R. and Babazadeh, H., 2020. "Numerical modeling of paraffin melting expedition with considering nanoparticles through wavy duct". *Journal of Molecular Liquids*, Vol. 305, p. 112807.

Nowruzi, H., Nourazar, S.S. and Ghassemi, H., 2018. "On the instability of two dimensional backward-facing step flow using energy gradient method." *Journal of Applied Fluid Mechanics*, Vol. 11, No. 1, pp. 241−256.

Pillai, A.L., Nagao, J., Awane, R. and Kurose, R., 2020. "Influences of liquid fuel atomization and flow rate fluctuations on spray combustion instabilities in a backward-facing step combustor". *Combustion and Flame*, Vol. 220, pp. 337–356.

Qian, Y., Harada, T., Fukui, K., Umezu, M., Takao, H. and Murayama, Y., 2007. "Hemodynamic analysis of cerebral aneurysm and stenosed carotid bifurcation using computational fluid dynamics technique". In *International Conference on Life System Modeling and Simulation*. Springer Berlin Heidelberg, pp. 292−299.

Salman, S., Talib, A.A., Saadon, S. and Sultan, M.H., 2019. "Hybrid nanofluid flow and heat transfer over backward and forward steps: A review". *Powder Technology*, Vol. 363, pp. 448−472.

Schmid, P., 2009. "Riccati-based flow control". *Centre National de la Recherche Scientifique*.

Sigalotti, L.G., Sira, E., Klapp, J. and Trujillo, L., 2014. *Environmental Fluid Mechanics: Applications to Weather Forecast and Climate Change*, Springer International Publishing, pp. 3−36.

Spalart, P.R. and Venkatakrishnan, V., 2016. "On the role and challenges of CFD in the aerospace industry". *The Aeronautical Journal*, Vol. 120, No. 1223, pp. 209−232.

Wang, B. and Li, H., 2016. "Pod analysis of flow over a backward-facing step forced by right-angle-shaped plasma actuator". *SpringerPlus*, Vol. 5, No. 1, pp. 1–19.

Wu, Y., Ren, H. and Tang, H., 2013. "Turbulent flow over a rough backward-facing step". *International Journal of Heat and Fluid Flow*, Vol. 44, pp. 155–169.

Yim, E., Shukla, I., Gallaire, F. and Boujo, E., 2019. "Optimal spanwise-periodic control for recirculation length in a backward-facing step flow". *arXiv preprint arXiv:1907.01774*.

Zambrano, H., Sigalotti, L.D.G., Klapp, J., Peña-Polo, F. and Bencomo, A., 2017. "Heavy oil slurry transportation through horizontal pipelines: experiments and CFD simulations". *International Journal of Multiphase Flow*, Vol. 91, pp. 130−141. ISSN 0301-9322.

7. RESPONSIBILITY NOTICE

The authors are solely responsible for the printed material included in this paper.